Standard and anisotropic EVMs for near-wall treatment
Poiseille or plane channel flow (i)

Eddy-Viscosity modelling

Two low-Reynolds eddy-viscosity closure are here compared. The studied EV-models, based on a two-equations turbulent viscosity definition in the k-ε formulation, are below summarized:

standard, Launder and Sharma, 1974 *LS74*	*non-linear, Craft et al., 1993* *CLS93*
tensor representation with **gradient approximation** Newtonian-like stress-strain relationship up to 1^{st} order term	tensor representation with ***kinematic*** **polynomial expansion up to 3^{rd} order terms** non-Newtonian stress-strain relationship
dependence from strain invariant	dependence from strain and vorticity invariants
	empirical expansion coefficients *calibration* with experiments and numerical data *physical consistency* conditions
isotropy of stress normal components	**anisotropy** of stress components
	built-in sensitivity to curvature and rotation effects

Plane Poiseille flow, problem statement

The chosen case is a plane Poiseille flow which defines a condition of fully developed turbulent flow that could be modelled introducing the following simplifying hypothesis within the RA-momentum equation components:
- velocity component derivatives along the channel axis-direction (x) equal to zero,
- non-zero pressure gradient along the channel axis-direction (x),
- non-zero axial velocity gradient normal to the wall (y).

The flow is in that case unidirectional and it could be characterized by the following mean flow properties:

$U_m = 1$, mean bulk velocity
$U_c = 1.16\ U_m$, centreline velocity
$\delta = 1$, channel half-width
$u\tau = (1/15.1)\ U_m = 0.0662$, global wall shear-velocity

$Re\tau = u\tau\ \delta/\nu = 180$, the friction Reynolds number
$Re_m = U_m\ 2\delta/\nu = 5600$, the bulk Reynolds number

The direct simulation of Kim et al. (1987) is regarded as highly accurate due to the very fine discretization level, and is here considered as a well-established reference solution for turbulence model assessment.

Plane Poiseille flow, numerical model

A particularly interesting feature of unidirectional flow problem in case of fully developed condition, is that it could be modeled isolating a portion of the flow field of elementary length.
A non-uniform grid distribution across the flow was used, with use of 101 nodes in the direction normal to the solid boundary (*y*). This grid refinement agrees with the grid independency analysis presented in literature (Pettersson et al., 1996). In the axial direction (*x*) where instead used 3 nodes, able to define a quadratic approximation on third-order accurate Q2/Q1 interpolation spaces. The computational domain has the following dimension:
δ in the direction normal to the wall (*y*),
$\xi/\delta = 0.01$ in the axial direction (*x*),
with the stretching toward the solid boundary set to $\delta'/\delta = 5.46\ 10^{-3}$.

The same set of boundary conditions was considered for the tested EVMs, consisting of no-slip conditions and homogeneous Dirichlet conditions for k and for the corrected dissipation rate at the wall. The fully developed flow under investigation is driven by an imposed pressure gradient:
$dp/dx = -\rho\ (u\tau)^2/\delta$,
which acts as a Neumann natural boundary condition on *x* momentum component.

A direct Crout-like solver was used, and the convergence threshold has been set equal to 10^{-9} for both the solution errors and its residual.

Plane Poiseille flow, results and discussion

The comparative investigation involved both integral as well as turbulent flow properties and quantities.

Integral flow properties

Table 1: Integral and mean flow properties

	DNS	*LS74*	*CLS93*
skin friction coefficient, C_f	8.18 10-3	12.6 10-3	10.6 10-3
displacement thickness, δ^*/δ	0.141	0.117	0.106
momentum thickness, θ^*/δ	0.087	0.0879	0.0819
shape factor, H	1.62	1.328	1.293
ratio U_c/U_m	1.16	1.175	1.163

It is worth to note that the skin friction data well behave with reference to the classical Dean's experimental correlation of $C_f = 0.073\ Re_m^{-0.25} = 8.44\ 10\text{-}3$. Furthermore, the ratio between the mean centreline velocity and the mean bulk velocity shows the fair agreement between DNS and CLS93 data.

Mean flow field data

The mean velocity distributions are plotted in Fig. 1 using linear scale and global coordinates, in Fig. 2 using semi-logarithmic scale and wall coordinates. While in Fig. 3 are plotted the turbulence kinetic energy profiles in the vicinity of the solid boundaries using wall coordinates.
The following conclusions could be drawn:

1. In Fig. 1, the CLS93 mean velocity profile agrees fairly with the DNS one, confirming the good prediction of mean velocity scales (U_c/U_m) shown in Table 1. In the vicinity of the solid wall the CLS93 profile predicts also velocity normal gradient closer to that computed by DNS.
2. In Fig. 2, the CLS93 confirms a better prediction of the viscous wall region (viscous sub-layer and buffer layer) up to $\delta^+ = 100$. Away from the wall the CLS93 profile flattening starts within the buffer layer (about $\delta^+ = 20$), thus anticipating the DNS one that begins the flattening about the end of buffer layer.
3. In Fig. 3, the CLS93 shows fair agreement with DNS profile within the viscous sub-layer (up to about $\delta^+ = 5$) and begin to markedly differ from the buffer layer region. Fig. 3 shows also that the CLS93 model fails to predict correctly the turbulence kinetic energy value according to the behaviour already mentioned by Launder (1996) discussing the model under-prediction of Reynolds stress normal components.

Reynolds stress components

In Fig. 4 normal Reynolds-stresses are plotted, and in Fig. 5 the shear Reynolds stress profiles is shown. Both the distributions refer to global coordinates. The following conclusions could be highlighted:

4. In Fig. 4, the already mentioned failure of non-linear model CLS93 is confirmed by the marked difference between the DNS and EVM prediction of u^+ (peak CLS93 value of 1.65, DNS peak value of 2.65), in terms also of position (peak CLS93 value in the viscous sub-layer, DNS peak value within the buffer layer). The same Fig. 4 shows clearly the anisotropy in the normal Reynolds stresses recovered by the CLS93 model. This behaviour is in clear agreement with the analysis provided by Launder (1996).
5. In Fig. 5, the profiles of Reynolds shear stress are compared. It is significant that although the under-prediction of Reynolds stress component normal to the wall, the CLS93 is able of predicting a more realistic shear stress distribution that is a fluid eddy viscosity closer to the DNS computation particularly within the viscous sub-layer.

Budget of turbulent kinetic energy

In Fig. 6 to Fig. 9 are compared the components of turbulent kinetic energy budget. Respectively: Fig. 6 the viscous diffusion; Fig. 7 the turbulent diffusion; Fig. 8 the production of k; Fig. 9 the dissipation rate. All the distribution are plotted using wall coordinates.

Standard and anisotropic EVMs for near-wall treatment
Poiseille or plane channel flow (i)

Plane Poiseille flow, results

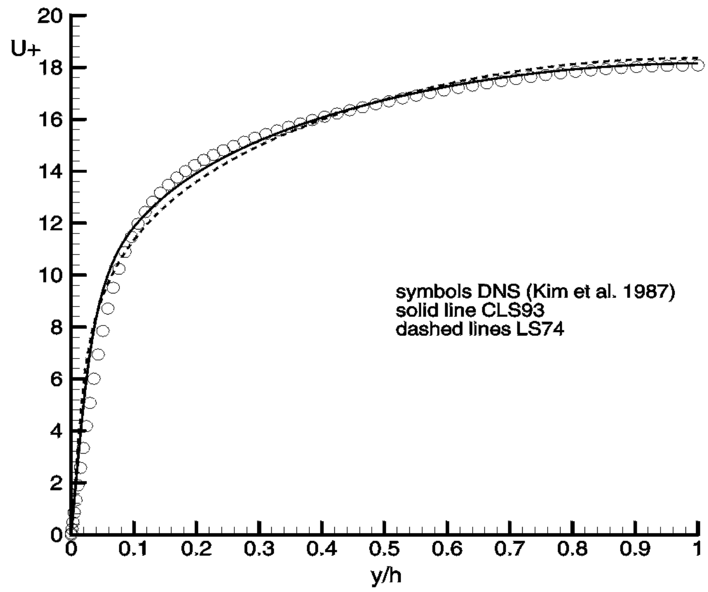

Fig. 1: mean velocity profiles in global coordinates

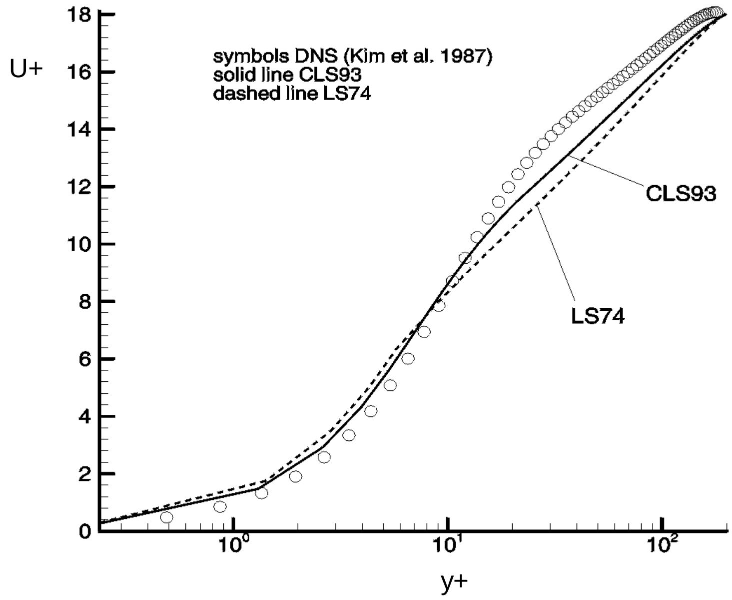

Fig. 2: mean velocity profiles in semi-logarithmic scale and wall coordinates

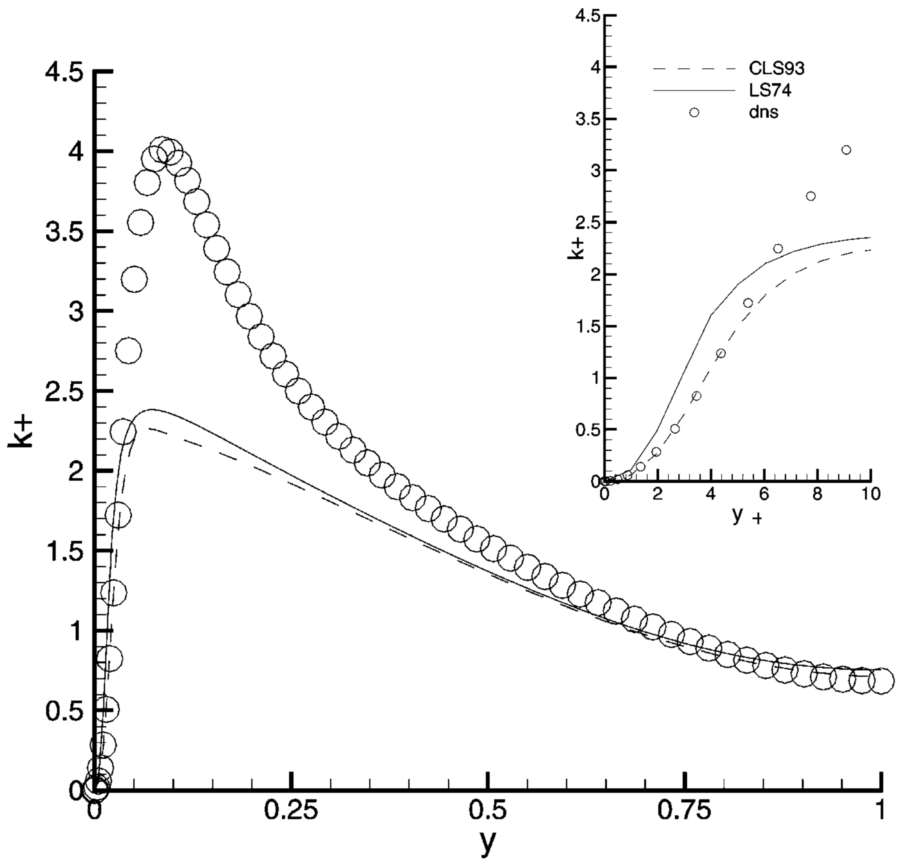

Fig. 3: turbulent kinetic energy profiles in global and wall coordinates (y+ range 0 ÷ 10)

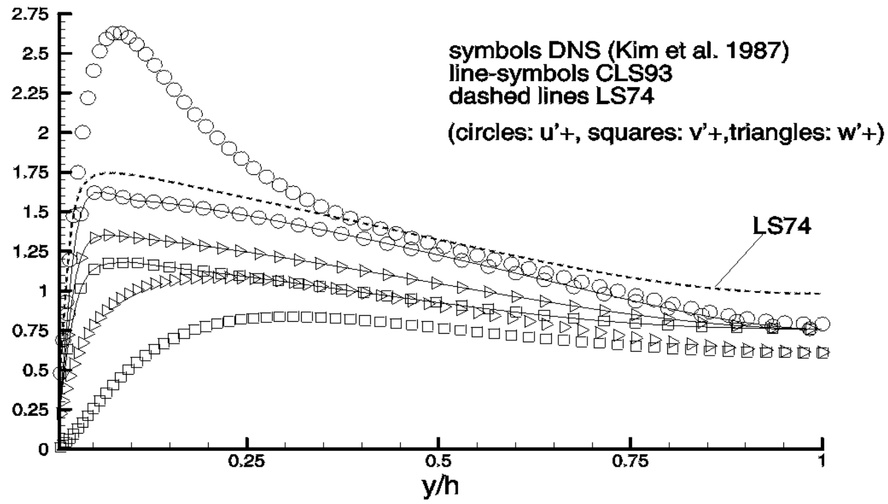

Fig. 4: Normal Reynolds stresses in global coordinates.

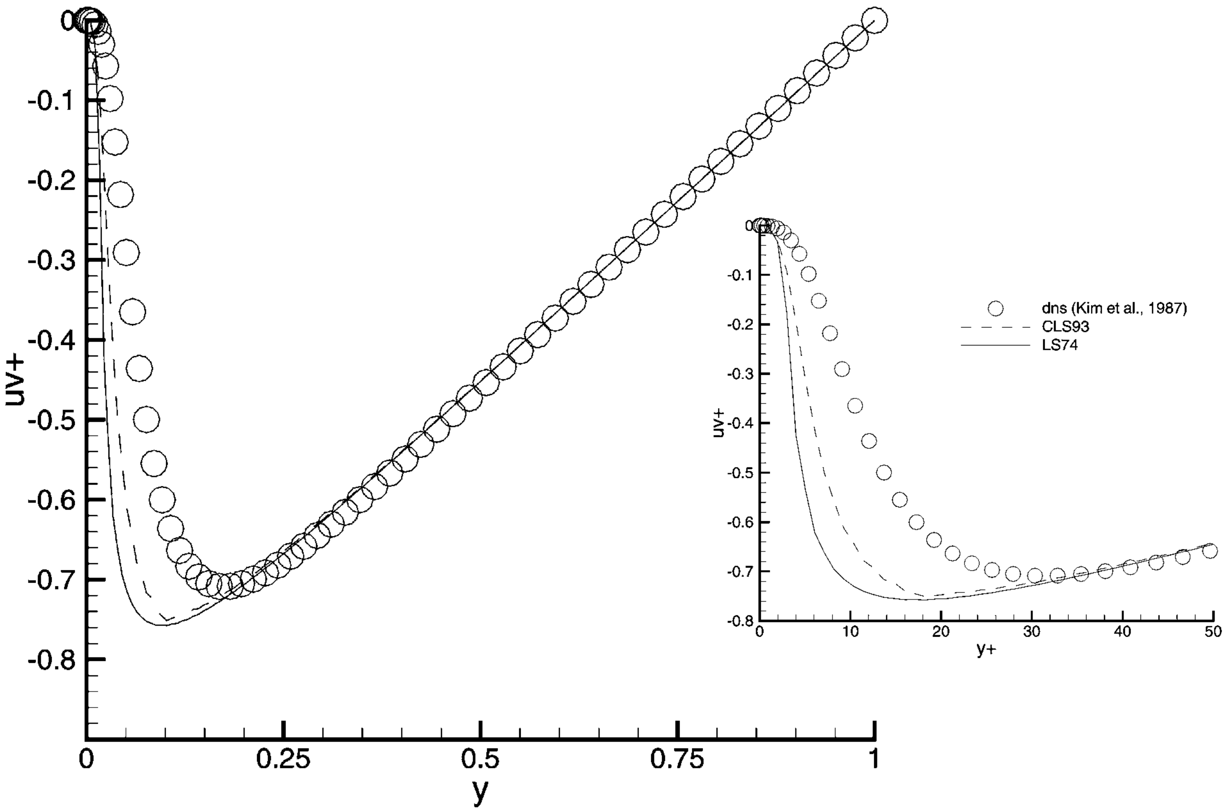

Fig. 5: Reynolds shear stress in global and wall coordinates (y+ range 0 ÷ 50)

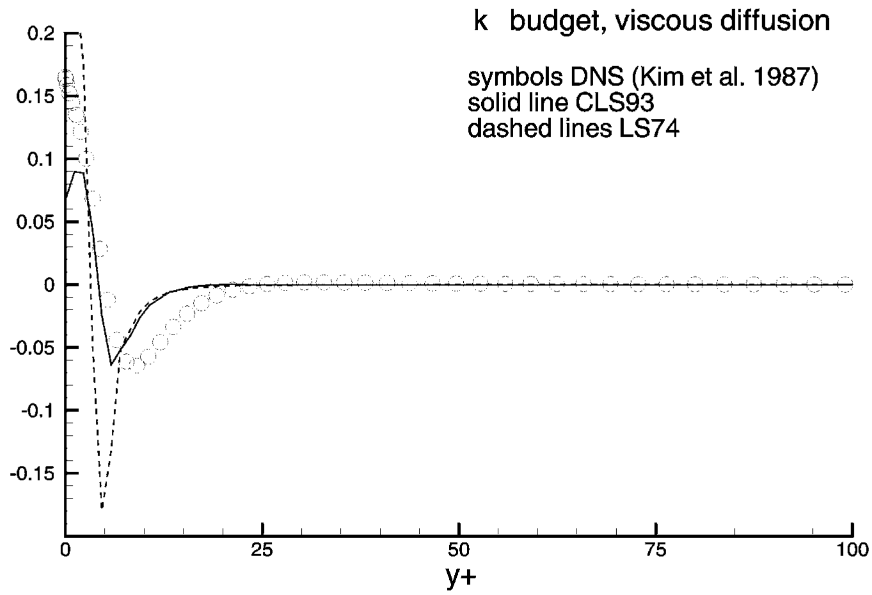

Fig. 6: *k* budget, viscous diffusion.

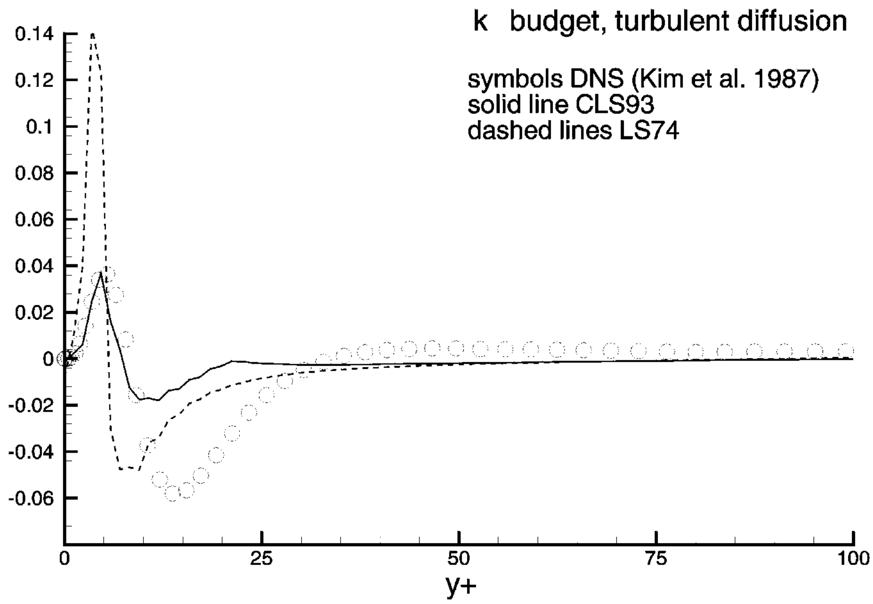

Fig. 7: *k* budget, turbulent diffusion.

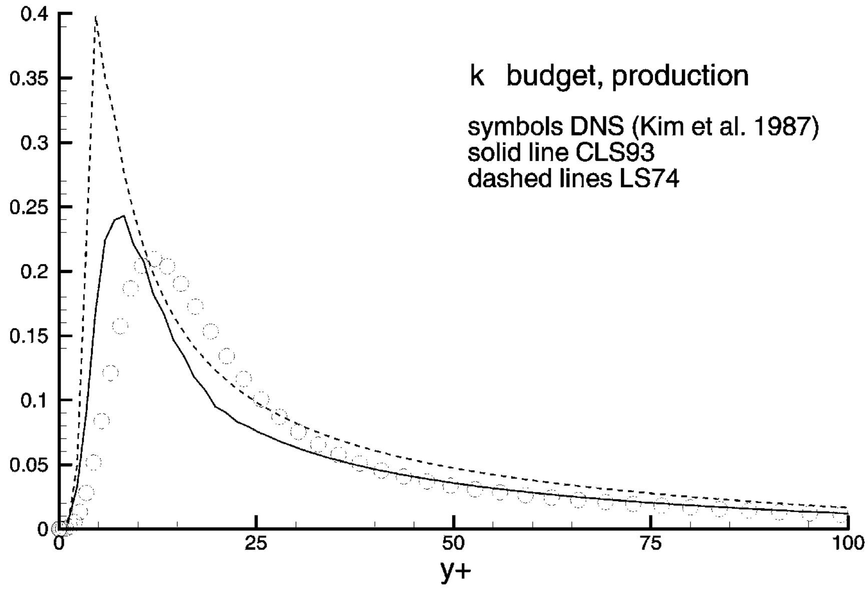

Fig. 8: *k* budget, production.

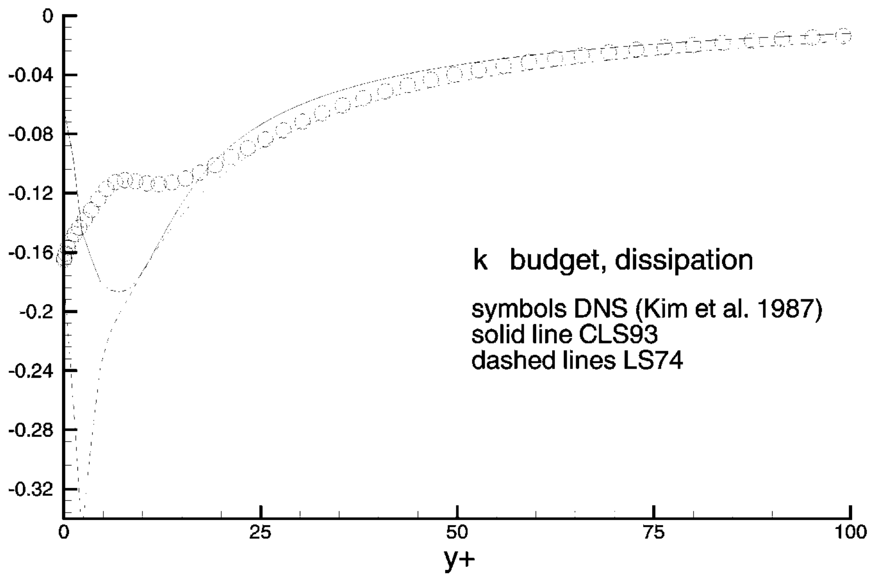

Fig. 9: *k* budget, dissipation.